

AD-A168 939

VISUALIZATION OF THREE-DIMENSIONAL FORCED UNSTEADY  
SEPARATED FLOW(U) FRANK J SEILER RESEARCH LAB UNITED  
STATES AIR FORCE ACADEMY CO H ROBINSON ET AL. 1986  
FJSRL-TJ-86-0007

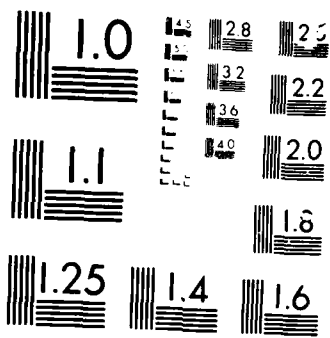
1/1

UNCLASSIFIED

F/G 20/4

NL





Mr. Robert J. ...

# AIAA'86

*(Handwritten mark)*

AD-A168 939

**AIAA-86-1066**

## **VISUALIZATION OF THREE-DIMENSIONAL FORCED UNSTEADY SEPARATED FLOW**

M. Robinson, H. Helin, Univ. of Colorado, Boulder, Co.

F. Gilliam, J. Russell, USAF Academy, Co.

J. Walker, F. J. Seiler Research Lab, USAFA, Co.

DTIC FILE COPY

DTIC  
ELECTE

JUN 3 1986

S

D

A

This document has been approved for public release and sale in its entirety and without limitation.

## **AIAA/ASME 4th Fluid Mechanics, Plasma Dynamics and Lasers Conference**

May 12-14, 1986/Atlanta, GA

# VISUALIZATION OF THREE-DIMENSIONAL FORCED UNSTEADY SEPARATED FLOW

M. Robinson\*  
Dept of Aerospace Engineering  
University of Colorado  
Boulder, Co., 80309

H. Helin\*\*  
Dept of Aerospace Engineering  
University of Colorado  
Boulder, Co., 80309

F. Gilliam\*\*\*  
Dept of Aeronautics  
USAF Academy  
Colorado Springs, Co., 80840-5831

J. Russell\*\*\*\*  
Dept of Aeronautics  
USAF Academy  
Colorado Springs, Co., 80840-5831

J. Walker\*\*\*\*\*  
Frank J. Sellar Research Laboratory  
USAF Academy  
Colorado Springs, Co., 80840-6528

Accession For	
NTIS GPO	<input checked="" type="checkbox"/>
DTIC TAB	<input type="checkbox"/>
Unannounced	<input type="checkbox"/>
Justification	
By	
Distribution/	
Availability Codes	
List	Avail and/or Special
A1	

## Abstract

Three-dimensional unsteady flow separation was visualized for a semi-infinite span wing pitched upward at a constant rate from 0 to 60° angles of attack. Initially, many of the same complex flow perturbations, including the formation of leading and trailing edge vortices observed from two-dimensional flow separation were evident. Using the semi-infinite wing, the flow field was further complicated by a wing tip vortex that developed orthogonal to the separation induced leading and trailing edge vortices. The tip flow distorted the development of the initially two-dimensional inboard, leading edge vortex. The simple pitching motion history permitted resolution of the development of individual vortices as a function of airfoil motion parameters. Also, vortex-vortex interactions were examined between separation-induced vortices and wingtip vortices. The interactions were characterized for time periods that extended well beyond the actual pitching motions.

## Nomenclature

c airfoil chord

k reduced frequency  $\omega c/2V_\infty$

\* Assistant Professor Adjunct, Department of Aerospace Engineering Sciences, Member AIAA  
1Lt., USAF, Graduate Research Associate, Department of Aerospace Engineering Sciences, Member AIAA

\*\* Lt., USAF, Associate Professor, Department of Aeronautics, Member AIAA

\*\*\* Maj., USAF, Assistant Professor, Department of Aeronautics, Member AIAA

\*\*\*\* Maj., USAF, Chief of Aeromechanics Division, FJSRL, Member AIAA

This paper is declared a work of the U.S. Government and therefore is in the public domain.

$R_e$  Reynolds number  $\rho V_\infty c/\mu$

$\bar{t}$  non-dimensional time  $t \cdot V_\infty/c$

$V_c$  convecting velocity of vortex center

$V_\infty$  free stream velocity

$\alpha^+$  reduced pitch rate  $\dot{\alpha} \cdot c/V_\infty$

$\dot{\alpha}$  pitch rate rad/sec

$\beta$  tip vortex streakline deflection angle

$\mu$  kinematic viscosity

## Introduction

The potential utilization of large scale vortices to enhance lift has provided much of the current research interest in unsteady aerodynamics<sup>1,2,3</sup>. Wakes created through forced unsteady flow separation are dominated by the presence of large scale leading and trailing edge vortical formations originating from the separated boundary layer vorticity<sup>4,5,6,7</sup>. In two-dimensional flows, vortices induced through airfoil pitching motions beyond static stall have been observed to create transient lift and moment coefficients four to five times larger than the maximum conventional steady state values.<sup>8,9,10,11,12</sup> Changes in any of the parameters affecting airfoil motion dynamics produced reliable alterations in vortex development and strength. Thus, many utilization schemes have been envisioned<sup>13,14,15</sup> which employ large scale vortices to enhance conventional airfoil performance. Yet, fundamental questions remain concerning the basic physics of vortex development and the validity of two-dimensional results in three-dimensional applications.



Flow fields resulting from forced unsteady flow separation are inherently complex due to the spacial and temporal interdependence of flow perturbations on airfoil geometry and motion history. In a two-dimensional test circumstance, where the airfoil motion is driven harmonically,<sup>4,5,6,7,8,9</sup> flow history effects from vortex-vortex interactions prevail. Vortex stacking produced by multiple airfoil oscillations at high oscillation rates (reduced frequencies >1.5) complicate the wake dominated flow field. Separating the effects of vortex-vortex interactions from vortex-airfoil influences and the dependence on different airfoil motion histories have only recently commenced.<sup>16</sup>

When three-dimensional separation is involved, the degree of complexity increases an order of magnitude. In three-dimensional forced unsteady separated flows, vortex stretching must be considered as an additional vorticity source along with three-dimensional vortex-vortex interactions between orthogonally positioned vortical structures. Such flow circumstances occur when a semi-infinite wing oscillates beyond static stall.<sup>17</sup> The separated leading edge vortex initiates along the airfoil span and is initially aligned perpendicular to the shedding wing tip vortex. Use of a three-dimensional body geometry, such as a delta wing,<sup>18</sup> or swept wing,<sup>19</sup> to produce unsteady flow separation may further complicate the flow with vortex alignment dependent upon body shape.

To help simplify present tests, a relatively simple constant pitch rate motion was selected as the forcing function of the unsteady separation. A single pitch motion between 0 and 60° permitted documentation of vortex initiation and development without the effects of hysteresis from multiple cycles. Variation in non-dimensional pitch rate between  $\alpha^+ = 0.2$  and 1.0 under duplicate test conditions showed the dependence of vortex formation on the airfoil motion dynamics. Further, the existence of previous flow visualization and pressure measures<sup>10,11,12</sup> for the two-dimensional cases at the same test conditions allowed direct comparison with these three-dimensional results.

The major complication in three-dimensional unsteady flow fields arises from the wing tip vortex associated with the finite wing. In two dimensions, vortex initiation and development can be treated as a scalar quantity with the addition of boundary layer vorticity enhancing the development of the separated leading edge vortex. In three-dimensional flows, the relationships between vorticity production and vortex generation are much more complex<sup>17,18</sup>. Additional vorticity accumulation and/or reduction through vortex stretching must be taken into account in addition to normal boundary layer diffusion processes. Development of orthogonal vortices from the leading edge and airfoil wing tip raise fundamental questions regarding flow development in the wing tip region. How the leading edge vortex terminates with the wing tip vortex, what allocation process distributes boundary layer vorticity between these vortices, what influence the dynamic forcing parameters exercise over vortex structure, and the effects of orthogonal vortex-vortex interactions on airfoil pressure distributions are only some of the important issues to be addressed. Only through a thorough understanding of vortex initiation,

development and interaction processes can the ultimate performance enhancement possibilities be realized.

The present experiments focus on the phenomenology of three-dimensional forced unsteady flow separation elicited from a semi-infinite wing under constant pitch. Flow visualizations from high speed 16 mm movies documented the genesis of vortex initiation and development. Comparison with flow visualizations of two-dimensional airfoils were possible since duplicate test conditions were used.

#### Methods

Experiments were conducted in the 2' x 2' low turbulence (<0.03%) subsonic wind tunnel at the University of Colorado. Free stream velocities were set with a reference pitot tube located in the test section. One side of the tunnel had been refitted with a glass wall to permit flow visualization.

An extruded hollow case NACA 0015 with 6" chord was used for the experiments. Two-dimensional results were obtained with an airfoil section which spanned the entire 2 ft. test area. Three-dimensional measures were made with a semi-infinite wing section which extended 12" from the tunnel wall. The low aspect ratio (2.0) airfoil was constructed with a flat end tip and a circular 6" disk on the opposite end, next to the tunnel wall. Both airfoils were pitched about the quarter chord with the pitch axis aligned perpendicular to the free stream flow.

Fundamental to the visualization approach was the delivery of a dense smoke sheet along selectable span locations<sup>20</sup>. A smoke wire constructed of 0.005 tungsten located 18" upstream of the leading edge was used to heat a coating of Roscoe fog fluid. An optimal voltage vs. tunnel free stream velocity was obtained through trial and error to obtain the greatest smoke density possible. The smoke wire was stretched across an 18" span normal to the airfoil pitch axis and attached to two 0.25" copper rods. Sliding the copper rods into and out of the test section permitted delivery of the smoke sheet at any selectable location along the span.

High speed movies documented the dynamics of vortex development from two separate, orthogonal vantage points. A 16 mm Locam II variable speed movie camera was operated at a frame rate of 200 Hz. All experiments were performed with a tunnel speed of 10 ft/sec which established a non-dimensional time between subsequent movie frames of 0.1 (where time was nondimensionalized on free stream velocity and airfoil chord). Eastman 4-X negative 16 mm film was exposed with a 50 mm Nikon camera lens set at an aperture of 2.8. Illumination was provided with two Strobrite stroboscopic flash units synchronized with the high speed camera. The single point source bulbs operated with a total duration of 7 usec and provided virtually instantaneous visualizations with each movie frame.

A programmable motion control system drove a d.c. stepping motor through a constant pitch motion for both the two-dimensional and three-

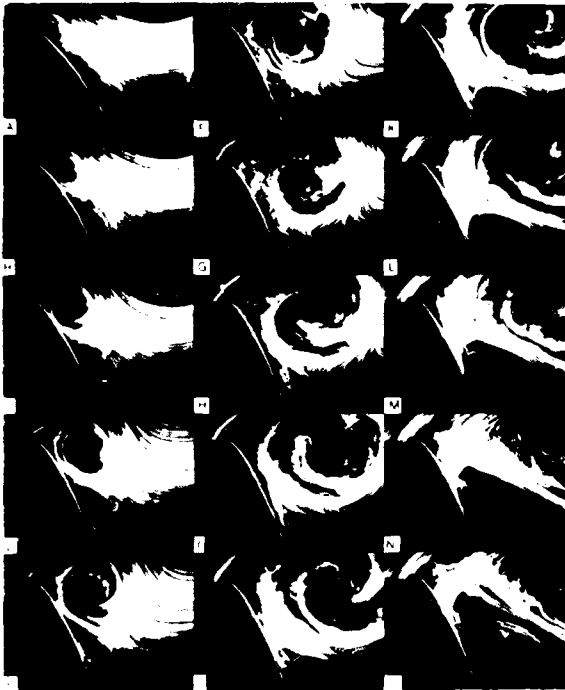


Fig. 1 Two-Dimensional Leading Edge Vortex Development From an Airfoil Pitched at Constant  $\dot{\alpha}$ ; NACA 0015;  $\alpha^+ = 0.6$ ;  $\Delta t$  between photographs of 0.2;  $\bar{V}_A = 1.5$  A-0 correspond to  $\alpha$ 's of 52.0, 56.9, 59.3, 60.0 ... 60.0°.

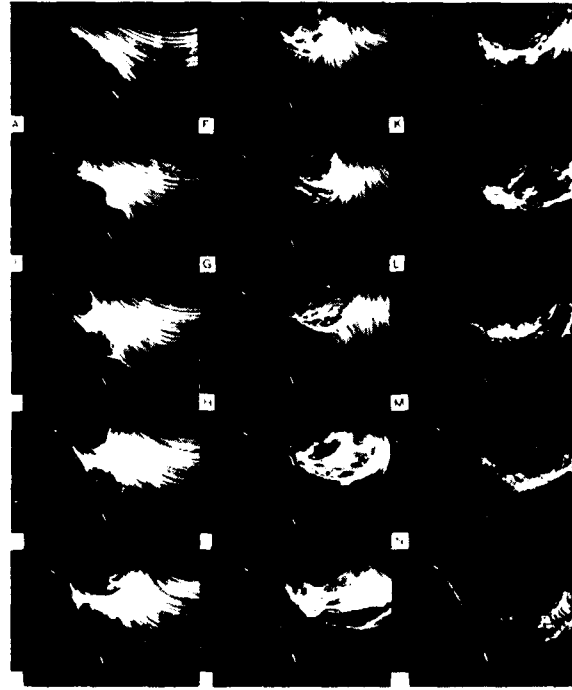


Fig. 2 Three-Dimensional Leading Edge Vortex Development From a Wing Pitched at Constant  $\dot{\alpha}$ ; NACA 0015;  $\alpha^+ = 0.6$ ; smoke wire location  $z/c = 1.0$ ;  $\bar{V}_A = 1.5$ ;  $\Delta t$  between photographs 0.2;  $\bar{V}_A = 1.5$ ; A-0 correspond to  $\alpha$ 's of 47.4, 54.2, 58.5, 60.0 ... 60.0°.

dimensional experiments. A 4 to 1 gear reduction between the stepper motor and airfoil pitch shaft provided a smooth ramp function through the pitch angles of 60°. Torque ranges to 3200 oz-in. permitted airfoil rotation rates up to 1145 deg/sec for the three-dimensional airfoil. Three rotation rates were used for this experiment; 229, 688, and 1145 deg/sec corresponding to non-dimensional pitch rates of 0.2, 0.6 and 1.0. All experiments were conducted at a chord Reynolds number of 23,000.

### Results

An inertial reference frame, fixed with respect to the wind tunnel was used to describe the three-dimensional flow field in the present studies. The origin of the orthogonal axes system was located on the leading edge of the wing tip with the wing at 0° angle of attack. The three axes were oriented as follows: 1) x-axis along the chord line parallel to the free stream flow, 2) y-axis perpendicular to the chord in the positive pitch direction and 3) the z-axis passing from the wing tip along the leading edge of the wing. Though the wing position changed with time, the coordinate system remained fixed relative to the tunnel reference system and the initial 0° angle of attack position of the wing. All positions are non-dimensionalized by the airfoil chord and represented as  $x/c$ ,  $y/c$  and  $z/c$ , respectively.

### Leading Edge Vortex Initiation and Development

When an airfoil is rotated in pitch beyond the static stall angle, a leading edge vortical complex is formed as the flow separates from the airfoil surface. Fig. 1 depicts the initiation and development of a leading edge vortex from the surface of a two-dimensional airfoil rotating at a constant pitch rate (non-dimensional pitch rate  $\dot{\alpha} = 0.2$ ) from 0 to 60° angle of attack. In Fig. 1, A, a vortex is clearly discernible about the airfoil leading edge at 52° angle of attack. The flow remained dynamically attached through angles of attack in excess of 46°, a full 30° beyond the steady state stall angle. Thus, separation was delayed due to the dynamic pitch motion of the airfoil section. This result agrees with other investigations using harmonic airfoil oscillations beyond static stall angles where stall was delayed during the upward pitch portion of the oscillation cycle.<sup>4,5,6</sup>

Subsequent photographs in Fig. 1 show the evolution of the dynamic stall vortex with increasing intervals of time. At a free stream velocity of 10 ft/sec, and camera frame rate of 200 Hz, the non-dimensional time (non-dimensionalized on  $V$  and airfoil chord) between movie frames was equal to 0.1. Thus, the non-dimensional time interval ( $\Delta t$ ) of 0.2 between consecutive photographs represents prints of every other movie

frame taken through the upward airfoil pitching sequence. By photograph D, the airfoil had reached maximum angle of attack and was stationary during the remainder of the visualization sequence.

Two distinct flow separation regions emerged on the airfoil upper surface during the vortex initiation phase of the motion. Immediately behind the leading edge vortex, a second vortex also with clockwise circulation formed between mid-chord and the trailing edge (Fig. 1, B-E). This vortex formation has been previously reported by McAllister and Carr<sup>7</sup> and Adler and Luttgies<sup>17</sup> using airfoils driven sinusoidally in pitch at either large oscillation angles ( $> 10^\circ$ ) or high oscillation rates ( $K > 2.5$ ). Walker, et al.,<sup>10</sup> also noted the large static pressure influence generated on the airfoil surface by this secondary shear layer vortex. After initiation, the larger leading edge vortex continued to convect over the airfoil chord and enveloped the entire airfoil surface. In the process, the secondary shear layer vortex was assimilated into the larger leading edge vortex and lost individual identity (Fig. 1, G).

As the dynamic stall vortex shed from the airfoil surface into the wake, a second vortex of counterclockwise circulation evolved from the trailing edge, underneath the leading edge vortex (Fig. 1, D). This trailing edge vortex rapidly grew in size, displacing the path of the leading edge vortex from a direction parallel to the free stream velocity to a path normal to the airfoil surface (Fig. 1, K-O).

Three separate and distinct periods of vortex development can be related to the single constant pitch airfoil motion history: 1) The forcing period where the airfoil experiences a rapid change in angle of attack, 2) initiation and development of the leading edge vortex and 3) the relaxation period where the induced vortices are permitted to develop and shed into the wake without additional external forces applied to alter the flow. The forcing period is characterized by the dynamic attachment of the flow during airfoil pitch and can be altered by the rate of pitch and angle through which the airfoil is driven. This time period would be visualized by a photographic series starting at zero angle of attack and ending just prior to vortex initiation (prior to Fig. 1, A). The initiation and development period for the leading edge vortex would subtend a period where the boundary layer separates from the airfoil surface (just prior to Fig. 1, A) and evolves into a discernible vortex (Fig. 1, B). The relaxation period encompasses the continuing development of the leading edge vortex as well as the initiation and development of the trailing edge vortex. Eventually, both the leading and trailing edge vortex complexes shed into the wake and the airfoil shows a quasi-steady bluff body shedding. Using these descriptions for the airfoil motion history, the three-dimensional unsteady separated flow field can be characterized and contrasted with the two-dimensional results in Fig. 1.

Initiation and development of a leading edge vortex from a semi-infinite wing possessed many of the same characteristics observed in the two-dimensional test cases described above. Fig. 2 shows a span-end view of the leading edge vortex development visualized with a smoke sheet introduced one chord inboard of the wing tip ( $z/c =$

1.0). These photographs were made using the same test conditions as the two-dimensional experiment (Fig. 1) and are sequenced with the same time increments between plates ( $V_\infty = 10$  f/sec;  $\alpha^+ = 0.6$ ;  $\Delta t = 0.2$ ). Thus, Figs. 1 and 2 may be contrasted directly, plate by plate, in order to ascertain differences in the resultant flow fields.

For the three-dimensional test case, a leading edge vortex was also formed during the initial forcing period. Initiation occurred at a slightly larger angle of attack ( $47^\circ$ , three-dimensional;  $41.5^\circ$ , two-dimensional) corresponding to a longer delay in time. Two shear vortices, rather than one (Fig. 2, B) appeared behind the leading edge vortex. The first vortex took residence between mid-chord and the trailing edge ( $x/c = 0.75$ , Fig. 2, B) while the second shed into the wake (Fig. 2, A-E). The major difference between the two test conditions, however, is the breakdown of the leading edge vortex in the three-dimensional test circumstance. Plates A-D (Fig. 2) show leading edge vortex development matching the two-dimensional test case. As the vortex approaches mid-chord (Fig. 2, F), the leading edge vortex no longer maintains simple two-dimensional characteristics. Smoke streaklines about the vortex circumference are displaced out of the original introduction plane of  $z/c = 1.0$  toward the wing tip (toward the viewing camera in these visualizations). Turbulent flow behavior with diffuse smoke patterns (Fig. 2, G-O) replace the cohesive, organized structure observed in the two-dimensional test. Also, the development of a trailing edge vortex observed in the two-dimensional tests was no longer evident.

The initial development and convection of the leading edge vortex for both the two-dimensional and three-dimensional conditions were very similar. Plotting the displacement of the leading edge vortex over the airfoil chord as a function of non-dimensional time, contrasts the behavior between two-dimensional and three-dimensional elicited vortices. In Fig. 3, non-dimensional pitch rates of 0.2 and 0.6 for the two-dimensional, and 0.2, 0.6 and 1.0 for the three-dimensional case are plotted. Again, the smoke sheet was introduced at mid-span for the two-dimensional model, and  $z/c = 1.0$  for the three-dimensional wing. The initiation time of the leading edge vortex ( $\bar{t}_1$ ) was defined by the first movie frame where a leading edge vortex was clearly discernible over the airfoil. All subsequent times are referenced to the leading edge vortex initiation time  $\bar{t}_1$ . Plotting vortex displacements in this manner permits examination of the vortex behavior independent of the airfoil motion history. The onset of airfoil motion with the airfoil at  $0^\circ$  angle of attack was used as the zero reference time base ( $\bar{t}_0$ ) for all test conditions.

Across test conditions, the initiation time of the leading edge vortex was delayed approximately  $\Delta \bar{t} = 0.2$  for the three-dimensional wing. After initiation, the vortices convected in a linear fashion downstream. Differences in the slopes of the displacement vs. time lines through the data points (thus, average convecting velocity) showed no appreciable change between the two-dimensional and three-dimensional tests. At non-dimensional pitch rates of 0.2 and 0.6, leading edge vortices convected at 0.35 and 0.45  $V_c/V_\infty$  respectively. For  $\alpha^+ = 1.0$  in the three-dimensional test, the

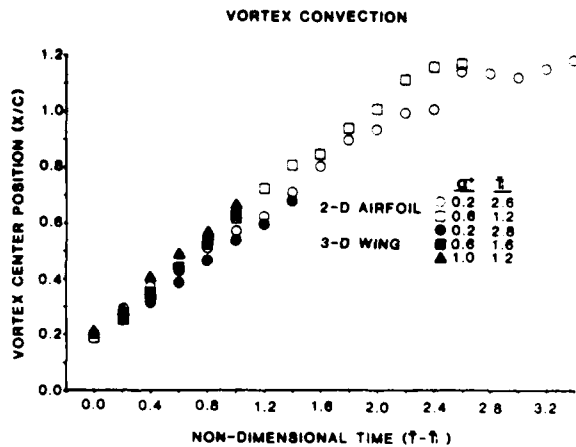


Fig. 3 Leading Edge Vortex Convection as a Function of Non-Dimensional Time; NACA 0015;  $\alpha^+ = 0.2, 0.6, 1.0$ ; smoke wire location  $z/c = 1.0$ ;  $\bar{t}_0$  corresponds to  $0^\circ$  prior to wing motion.

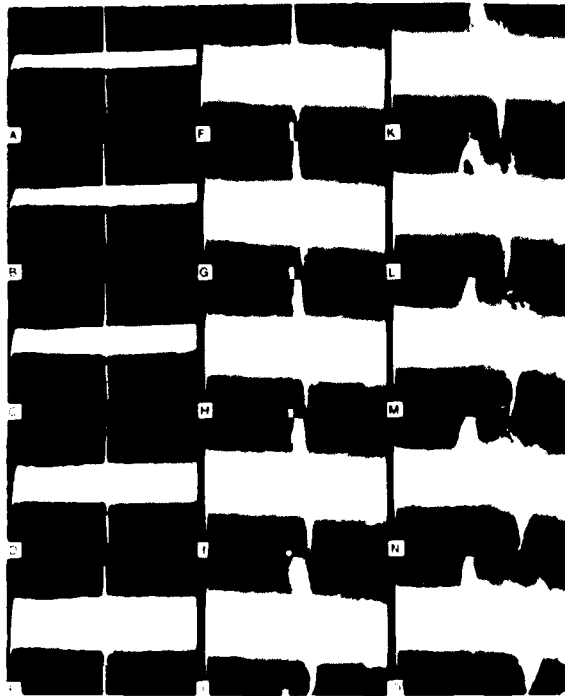


Fig. 4 Trailing Edge View of Leading Edge Vortex Development from a Three-Dimensional Wing Pitched at Constant  $\alpha^+$ ; NACA 0015;  $\alpha^+ = 1.0$ ; smoke wire location  $z/c = 0.8$ ;  $\bar{t}$  between photographs of 0.2;  $\bar{t}_A = 0.2$ ; A-O correspond to  $\alpha^+$ 's of 1.0, 5.3, 14.5, 37.3, 39.2, 49.8, 56.4, 60.0 ... 60.0°.

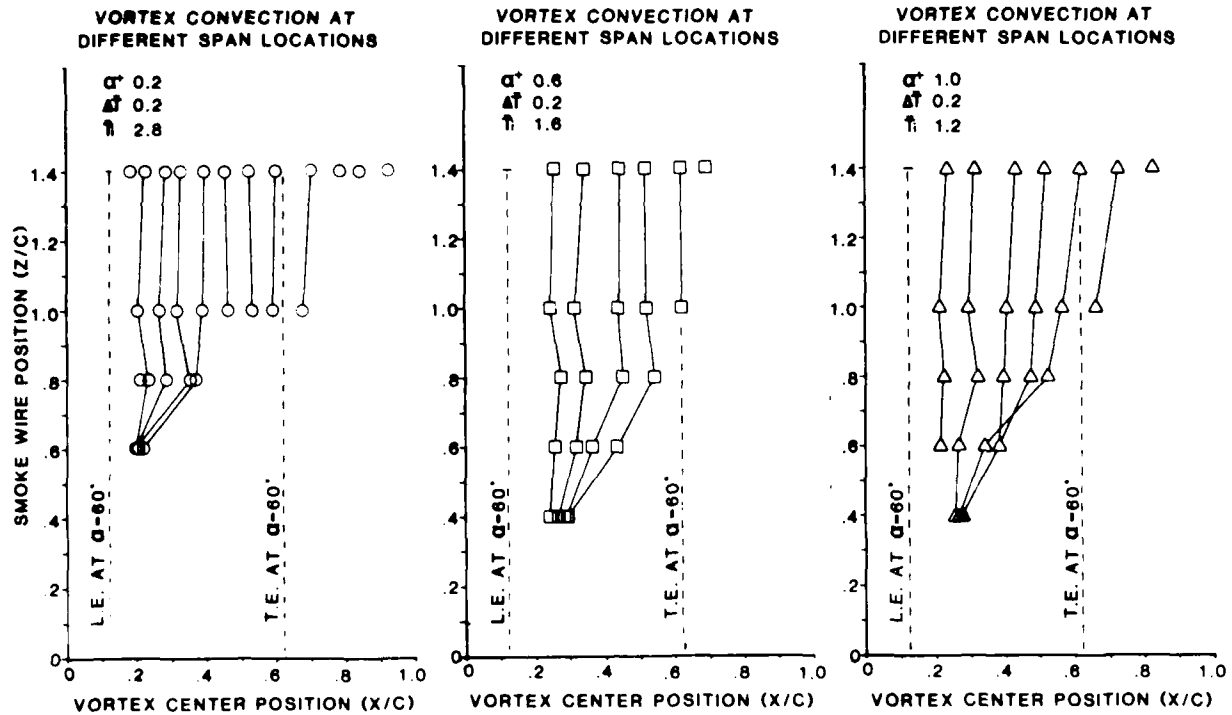
convection rate remained constant at  $0.45 V_c/V_\infty$ . In the three-dimensional test cases, vortex positions were plotted only where the leading edge vortex remained two-dimensional. The last data point indicates where two-dimensional behavior breaks down. Larger non-dimensional pitch rates produced an earlier breakdown in the leading edge vortex with the smoke sheet introduced at  $z/c = 1.0$ .

#### Three-Dimensionality of the Leading Edge Vortex

The three-dimensional breakdown of the leading edge vortex can be readily observed from an orthogonally located camera view of the pitching sequence. Whereas Fig. 2 examined the span-end view of the initiation and development process, Fig. 4 documents the three-dimensional breakdown from a viewing vantage point above and behind the airfoil trailing edge. White reference "tic" marks along the leading and trailing edge of the wing are evenly spaced in 0.2 chord increments ( $z/c = 0.2$ ). The first reference mark positioned to the right of the wing tip marked an interval of 0.1 c. For this sequence of photographs, the smoke sheet (coming directly at the camera lens in the center of Fig. 4, A) was introduced at the  $z/c = 0.8$  span location on the wing. Again, the non-dimensional time ( $\Delta \bar{t}$ ) between consecutive plates is 0.2. Photograph A in Fig. 4 was exposed at a reference time of 0.2 after the airfoil motion commenced (mean angle  $1^\circ$ ). With a non-dimensional pitch rate of 1.0, the semi-infinite wing attained maximum angle of attack ( $60^\circ$ ) in plate H.

From this vantage point, the three-dimensional displacement of the initially two-dimensional smoke sheet can be resolved. As the wing pitches toward maximum angle (Fig. 4, A-F), the smoke sheet passing below the wing surface moved toward the wing tip (Fig. 4, I) while the upper surface smoke near the trailing edge was displaced inboard, away from the tip. Note, however, that only minor displacements occurred during this segment of the rotation (Fig. 4, A-I) though the airfoil attained an angle of  $60^\circ$ .

The initial formation of the leading edge vortex was accomplished in nearly a two-dimensional fashion. Fig. 4, photographs F-K depict the initial time of formation and development of the leading edge vortex. As the vortex convected over the wing, the upper surface smoke sheet outlining the leading edge vortex was drawn toward the wing tip to a position of  $z/c = 0.6$ , a distance of 0.2 c from the original smoke sheet plane. At this new span location ( $z/c = 0.6$ ), the leading edge vortex remained outlined by the upper surface smoke sheet, yet, did not appear to convect further downstream toward the camera (Fig. 4, O). This span-wise convection of the leading edge vortex was apparent for all smoke introduction planes where  $z/c < 1.0$  from the tip. At  $z/c = 1.4$ , the leading edge vortex shed from the upper surface into the wake without exhibiting span-wise convection toward the tip. In the previous figure (Fig. 3), it was noted that the last position plotted for the semi-infinite wing data indicated where three-dimensional breakdown of the leading edge vortex occurred. The flow conditions exhibited in Fig. 4, H would have been considered the onset of three-dimensionality in the leading edge vortex and no further positions would have been plotted in Fig. 3



Figures 5, 6, and 7 Leading Edge Vortex Convection at Different Span Locations:  $\alpha^+$  values 0.2, 0.6, and 1.0 respectively; NACA 0015;  $\Delta \bar{t}$  between successive lines 0.2;  $\bar{t}_i$  2.5, 1.6, and 1.2.

for this test sequence.

Disparate "fingers of smoke" also appeared to the right of the leading edge vortex (Fig. 4, K-M) and extended out from the airfoil surface. Upon closer examination, these "smoke fingers" outlined the leading edge vortex at the original chord position where the smoke sheet was introduced ( $z/c = 0.8$ ). The leading edge vortex outlined by the disparate smoke at  $z/c = 0.8$  continued to convect downstream over the chord while rapidly increasing in diameter (Fig. 4, K-0).

The leading edge vortex convection was plotted for different smoke sheet introduction planes along the span. Figs. 5, 6 and 7 show the leading edge vortex convection behavior for non-dimensional pitch rates of 0.2, 0.6 and 1.0 respectively. Again, only the time and position points were plotted where the leading edge vortex demonstrated two-dimensional development without span-wise convection. These data were collected from span-end view movie frames similar to those printed in Figs. 1 and 2. The non-dimensional time increment between successive position points was equal to 0.2 (every other movie frame). Connected data points between different span locations show leading edge vortex positions at various spanwise locations at the same reference times. Thus, each successive line shows the convective behavior of the leading edge vortex along the span of the wing.

Vortex initiation occurred at the same point in time along the span of the wing. The initiation

times referenced to the onset of airfoil motion ( $\bar{t}_i$ ) were 2.8, 1.6, and 1.2 for non-dimensional pitch rates of 0.2, 0.6 and 1.0 respectively. Initially, the leading edge vortex line convected downstream in a two-dimensional fashion indicated by the straight line through the position data. At later times, the vortex line away from the tip ( $z/c \geq 1.0$ ) continued to convect in a uniform fashion parallel to the airfoil span. Near the tip ( $z/c \leq 0.8$ ), the leading edge vortex convection was arrested. At span locations of  $z/c = 0.4$ , the leading edge vortex remained stationary over the wing surface. Within this region, one test condition (Fig. 7,  $\alpha^+ 1.0$ ,  $z/c 0.6$ ) shows the leading edge vortex reversing direction and traveling upstream a short distance just prior to exhibiting three-dimensionality.

Two-dimensionality of the leading edge vortex line persisted for much greater periods of time at span locations furthest from the tip ( $z/c > 1.0$ ). At low non-dimensional pitch rates ( $\alpha^+ 0.2$ ) two-dimensionality persisted nearly twice as long away from the tip ( $z/c 1.4$ ) than near the tip itself. Larger  $\alpha^+$  rates produced similar behavior with vortex breakdown occurring first near the tip and propagating out from the tip along the vortex line.

#### Wing Tip Vortex Interaction

Near the wing tip, the flow field above the airfoil surface was dominated by the development of the wing tip vortex. In Figs. 5, 6, and 7, span locations less than  $z/c < 0.4$  showed no formation

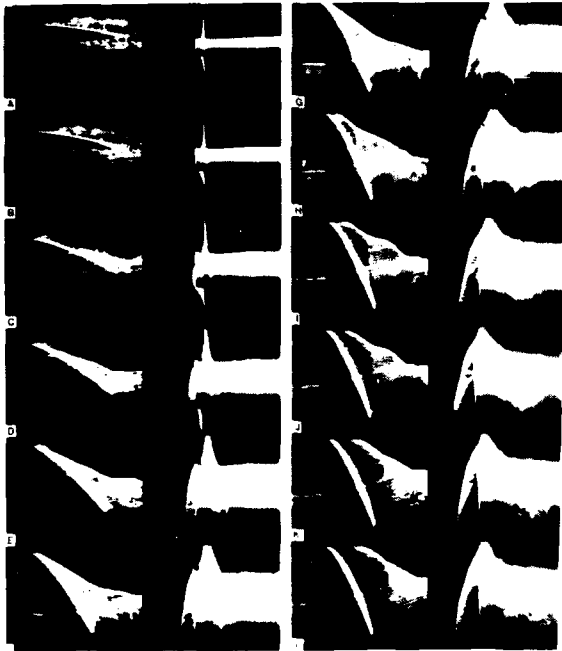


Fig. 8 Orthogonal Views of Wing Tip Vortex Development: NACA 0015;  $\alpha^+$  0.6; smoke wire location  $z/c = 0.1$ ;  $\Delta t$  between photographs of 0.3;  $\tau_A = 0.1$ ; A-L correspond to  $\alpha$ 's of 0.4, 1.5, 12.0, 24.6, 35.0, 47.5, 56.0, 60.0 ... 60.0°.

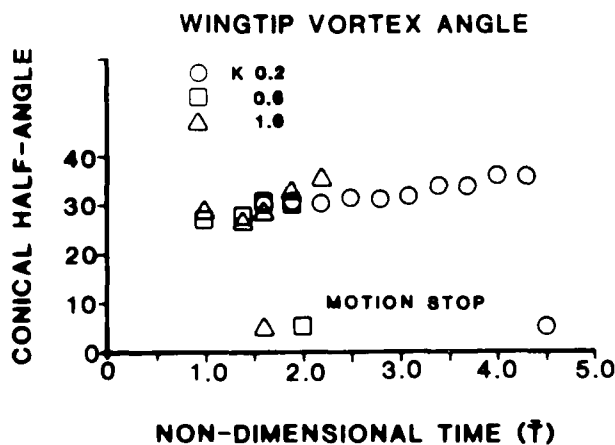


Fig. 9 Development of the Wing Tip Vortex Beta Angle as a Function of Non-Dimensional Time: NACA 0015;  $\alpha^+$  0.2, 0.6, 1.0; smoke wire location  $x/c = 0.1$ ;  $\tau_0$  corresponds to airfoil at 0° prior to wing motion.

of the leading edge vortex. Fig. 8 shows the span-end view along with the orthogonally positioned trailing edge perspective side by side. The smoke sheet was released upstream of the wing tip at the  $z/c = 0.1$  c span location. This sequence depicts flow development about the tip at a non-dimensional pitch rate of 0.6. Consecutive photographs are incremented in 0.3 time steps (every third movie

frame) with plate A in Fig. 8 at a mean angle of 0.42°, reaching 60° in plate H.

The smoke sheets above and below the wing tip were displaced along the span ( $z$  axis) as the wing pitched toward maximum angle of attack. On the upper surface, the smoke sheet was displaced away from the tip. Simultaneously, smoke from beneath the airfoil passed over and around the wing tip. From the trailing edge view (Fig. 8, plates A-F) a clear separation line is evident between the displaced smoke sheet on the upper surface and the smoke curling about the wing tip from the lower surface. The smoke sheet from beneath the wing tip envelops the wing tip vortex tracing a conical shape focused to a point at the tip of the leading edge. The influences traced by the two smoke sheets are clearly separated into distinct regions where smoke from the lower surface dominates the flow within the immediate wing tip region while flow on the upper surface is canted away from the tip.

A portion of the smoke sheet on top of the wing near the surface of the leading edge was drawn toward the wing tip. Fig. 8, plates A-F show the upper surface smoke displacement toward the tip of the leading edge. An intersection line exists starting at the leading edge tip proceeding down the chord at an angle of 30° to the wing tip. This intersection line separates the influence of the wing tip vortex flow from the flow over the upper surface. At later periods in the development phase (Fig. 8, G-L), this intersection line from the leading edge lifts from the airfoil surface, no longer adhering to the wing surface contour. For all three  $\alpha^+$  conditions tested (0.2, 0.6, 1.0), a strong temporal correlation existed between three separate events: 1) The leading edge vortex at  $z/c = 1.4$  (furthest measured point away from the tip) shed from the airfoil surface, 2) three-dimensionality within the leading edge vortex developed along the span, and 3) the intersection line separating the two regions of wing tip and upper surface flow began to shed from the wing surface.

Previous experimental investigations<sup>17,19</sup> have used the  $\beta$  angle to characterize wing tip flow. Flow passing from beneath the wing traces the wing tip vortex in a helical arc around the wing tip and into the wake. The  $\beta$  angle measured the intersection made by the helical arc with the chord line of the tip itself. The greater the  $\beta$  angle, the larger the differential pressure effects about the tip. For these results, the  $\beta$  angle remained constant at 90° from the onset of pitch through the period where the interaction region began to shed. As a second measure, the conical half-angle traced by the wing tip flow and the chord line were also measured (Fig. 9) for the same time period. Across both non-dimensional pitch rates and time, this angle maintained a relatively constant value of 30°.

#### Discussion

Though the three-dimensional forced unsteady separated flow about a semi-infinite wing was inherently complex, several well-defined flow perturbations were identified with counterparts observed in two-dimensional results. The flow field was dominated by the development of a leading edge vortex elicited from the separated flow as the

wing pitched beyond the static stall angle. In addition, a second orthogonally positioned vortex emanated from the wing tip. Both flow structures dominated the potential flow field within localized areas of the wing and appeared to elicit vortex-vortex interactions near the intersection region between the two vortices. Vortex initiation and development was extremely repeatable across test conditions permitting analysis via flow visualization. Introduction of smoke sheets at various span locations permitted resolution of both the two-dimensional and three-dimensional behaviors of the flow field along the span. The flow development can best be described in terms of three separate phases of the airfoil motion history: 1) vortex initiation during the pitching or forcing period of wing motion, 2) vortex development and interaction as the airfoil motion approached maximum angle of attack and 3) the relaxation period where airfoil motion ceased and the vorticity from the wing surface shed into the wake.

#### Vortex Initiation - Forcing Phase

Leading edge vortex initiation followed qualitatively, the same general patterns observed for two-dimensional airfoils undergoing similar pitch motions,<sup>10,11,16</sup> airfoils oscillating sinusoidally in pitch,<sup>4,5,6,7</sup> and semi-infinite wings oscillated in pitch beyond static stall.<sup>17,19</sup> Increases in the non-dimensional pitch rate delayed leading edge vortex development to later times in the motion history. Initiation of the leading edge vortex remained two-dimensional along the span. It is interesting to note, however, that near the wing tip ( $z/c < 0.4$ ) a leading edge vortex failed to develop.

During the forcing period, the region near the wing tip ( $z/c < 0.4$ ) was completely dominated by the development of the wing tip vortex. Formation of the wing tip vortex began immediately as the wing pitched from  $0^\circ$  angle of attack. A clear distinction could be made between the allocation of smoke to the wing tip as opposed to the upper surface flows. Smoke introduced below the airfoil surface near the tip was entrained up and around the airfoil tip into the wing tip vortex. In contrast, smoke over the upper (suction) surface introduced in the same span plane near the tip was displaced away from the tip as it moved over the chord. A clear separation emerged as a distinct intersection line defining the two zones of pressure vorticity influence. That from the lower (pressure) surface formed the wing tip vortex whereas upper (suction) surface vorticity remained concentrated in the leading edge vortex. Unlike previous results using oscillating semi-infinite wings,<sup>17,19</sup> the geometric angle describing the vertical shape of the wing tip vortex remained constant through the pitching portion of the motion history.

#### Vortex Development and Interaction Phase

Though initially forming as a two-dimensional line vortex along the span at  $x/c < 0.2$ , the leading edge vortex and its nominal convection behavior was quickly altered by the influence of the wing tip vortex. Prior to the onset of three-dimensionality in the leading edge vortex, the leading edge vortex convected in a two-dimensional line along the span of the airfoil (Figs. 5, 6, 7) at span locations greater than 0.8c away from the

tip. The averaged convection rate correlated well with previous two-dimensional airfoil results of leading edge vortex development (Fig. 3). Near the wing tip ( $0.4 < z/c < 0.8$ ), convection of the leading edge vortex was slowed while at span locations less than 0.4c, the leading edge vortex appeared stationary and did not convect before three-dimensionality occurred.

Previous work by Adler and Lutges<sup>17</sup> with an oscillating semi-infinite wing had shown similar results in convecting behavior. At span locations greater than 1.0c away from the tip, the leading edge vortex development showed no discernible three-dimensionality and the convection rate appeared the same as observed for a two-dimensional airfoil oscillated in pitch under the same test conditions. For the conditions reported here, a small influence in convection was evident at span positions up to 1.0c from the tip. However, by 1.4c, the leading edge vortex convected in a two-dimensional fashion over the wing without displacement toward the tip.

#### Vortex Shedding - Relaxation Phase

Correlation between the shedding of the two-dimensional leading edge vortex at span positions greater than 1.0c and the separation of the wing tip interaction region suggests a strong link between the leading edge and wing tip vortex. Previous work for two-dimensional airfoils has shown that "cataclysmic" stall results when the leading edge vortex sheds from the airfoil surface. From visualization results,<sup>4,5,6,7</sup> a trailing edge vortex forms with shedding of the leading edge vortex and flow completely separates from the airfoil surface. This separation is also reflected in pressure measurements made along the airfoil surface.<sup>8,9,10,11,12</sup> In the results reported here, a trailing edge vortex was not observed near the tip, although separation of the leading edge / wing tip vortex interaction region does occur.

For a semi-infinite wing, the bound vorticity contained around the wing must continue in a line through the wing tip vortex. The wing tip vorticity reflecting the magnitude of the lift generated by the wing. Previous pressure measurements on two-dimensional airfoils have shown that shedding of the leading edge vorticity away from the wing triggers a substantial loss in lift.<sup>8,9,10,11,12</sup> In the visualizations reported here, shedding of the leading edge vortex is also commensurate with separation of the wing tip interaction region from the wing surface. This loss in lift appears to trigger separation of the wing tip vortex so that the wing tip vortex and bound vorticity near the leading edge at the wing tip ( $z/c < 0.4$ ) may separate together in a continuous line.

Though these results are preliminary, some speculation can be made regarding the nature of the three-dimensionality arising in leading edge vortex development. From pressure measurements on two-dimensional airfoils at similar test conditions, pressure distributions about pitching airfoils can produce lift coefficients much greater than steady state values.<sup>8,9,10,11,12</sup> The low static pressure distributions which yield these values of  $C_L$  are produced from the leading edge vortex development and convection over the airfoil surface. In the

three-dimensional test case, this added lift must be reflected in an enhanced wing tip vortex. Development of the stronger wing tip vortex ultimately appears to draw the two-dimensional development of the leading edge vortex out of plane toward the tip. In the results reported by Adler and Luttgies for an oscillating wing, three-dimensionality was limited to a region within  $1.0c$  of the wing tip, whereas the present results extend the region to  $1.4c$ . This difference may also be related to the differences in  $C_p$  values produced for the two different motion histories. Two-dimensional airfoil results from an oscillating airfoil produce  $C_p$  values roughly one-half the value of those reported by Walker, et al.,<sup>10,11</sup> and Jumper, et al.,<sup>21</sup> for two-dimensional airfoils pitched at constant rates to large angles of attack.

After the leading edge vortex shed into the wake, flow field development about the three-dimensional wing appeared to be quite different from the behaviors observed in two-dimensional airfoil results.<sup>16</sup> Shedding of the leading edge vortex from the two-dimensional airfoil elicited a trailing edge vortex of opposite circulation. Growth of the trailing edge vortex appeared to "re-direct" the separated shear flow from the airfoil leading edge into a second leading edge vortex. The growth and shedding of the second leading edge vortex closely paralleled the development of the first, however, shedding of the second leading edge vortex elicited a second, much weaker, trailing edge vortex. This process continued until a series of three to four secondary leading and trailing vortices had been produced. Integrated pressure measurements by Jumper, et al.,<sup>21</sup> clearly reflect the development of these secondary vortices in the lift coefficient plots as a function of non-dimensional time. Each successive leading edge vortex produced a diminished pressure effect compared to the previous vortex. After three to four damped pressure peaks, the lift coefficient had decayed to approximately nominal steady state values.

In the three-dimensional wing results, a trailing edge vortex does not develop near the wing tip. The interactive leading edge / wing tip vortex region separated and shed from the wing without eliciting any additional vortical structure. At span positions one chord from the tip ( $z/c = 1.0$ ) a second leading edge vortex development was observed during the relaxation phase. This second vortex development, however, did not arise from the growth of a trailing edge vortex. Shedding of the first leading edge vortex failed to produce the trailing edge vortex development observed in the two-dimensional airfoil results. Shedding of the second leading edge vortex however, did initiate a trailing edge vortex. The initiation and development of the second leading edge vortex and subsequent generation of a trailing edge vortex were not reflected in the wing tip flow. After separation of the first leading edge-wing tip vortex interaction, no further initiation or reattachment of flow about the wing tip was observed.

### Conclusions

Forced unsteady separated flow elicited from a semi-infinite wing pitched at a constant rate

through large angles of attack produced highly repeatable three-dimensional vortical wakes. These well-behaved vortex structures were readily resolved using smoke sheets introduced at various span positions, illuminated stroboscopically, and recorded with a high-speed movie camera.

The separated leading edge and wing tip vortices dominated specific regions of the wing surface. Similar to the results reported earlier for oscillating airfoils,<sup>17</sup> the wing tip vortex dominated the local flow about the tip ( $z/c < 0.4$ ) and exercised influence over the development of the leading edge vortex in the tip region ( $0.4 < x/c < 1.4$ ). Leading edge vortex development at distances greater than  $1.4c$  from the tip appeared unaffected by wing tip influences. Vortex initiation, development and convection rates at these span locations matched those of two-dimensional airfoil results. Thus, three-dimensional effects from a wing under constant pitch were observed at distances 40% greater than for the oscillating wing case.

Though these results are qualitative, some speculation can be made regarding the validity of two-dimensional results in predicting the performance of three-dimensional bodies. The initial similarity in leading edge vortex development between two-dimensional and three-dimensional test results suggests that existing two-dimensional pressure measurements may be appropriate to help predict sectional aerodynamic coefficients for semi-infinite wings. Of course, such measurements would be restricted to span locations away from the tip. At later periods in the relaxation phase, initiation and development of subsequent leading and trailing edge vortical flows appear substantially different between the two-dimensional and three-dimensional test circumstances. Previous two-dimensional results may not be particularly useful in describing flow interactions that occur during such relaxation phases.

As noted earlier, the present work does provide some insight into orthogonal vortex interactions. Also, the above observations suggest a scheme for the vorticity allocations to leading edge and wing tip vortices. These two prominent vortex generation sites have little in common either spatially or temporally. Wing tip flow emanated from the lower boundary layer vorticity on the pressure surface. The wing tip vortex was established almost immediately with the onset of airfoil motion, and maintained a stable geometric size and shape through the forcing period. In contrast, multiple vortex initiation sites along the chord were observed from the upper surface boundary layer vorticity. Ultimately, only the leading edge vortex dominated the upper surface flow field. The vorticity allocation to the leading edge vortex remained clearly separated from the wing tip vorticity. Unlike the wing tip vortex, the leading edge vortex showed a continual vorticity influx, reflected in the rapid growth and convection of the vortex over the wing. Only at the intersection of the two sites of vortex generation was the interaction between the wing tip and leading edge vortices most prominent with the leading edge vortex exhibiting the greatest altered effects.

The present studies show enough reliability in

both the temporal and spacial arrangement of vortices, that full quantification of these vortical dynamics should be possible. Measures of pressure distributions as well as velocity profiles should reveal how the vortices are initiated and developed. And, such future studies should reveal critical facets of vortex-vortex interactions in these complicated unsteady flow fields.

#### Acknowledgments

This work has been sponsored by the U.S. Air Force Office of Scientific Research, WU-2307-F1-38, Dr. Jim McMichael, Project Manager. The assistance of Dr. Marvin W. Luttges was greatly appreciated. Manuscript prepared by S. Walts.

#### Bibliography

1. McCroskey, W.J., "Unsteady Airfoils," Annual Review of Fluid Mechanics, 1982, pp. 285-311.
2. McCroskey, W.J., "Some Current Research in Unsteady Fluid Dynamics," The 1976 Freeman Scholar Lecture, J. Fluids Engr., Vol. 99, 1977, pp. 8-38.
3. Carr, L.W., "Dynamic Stall Progress in Analysis and Prediction", AIAA Paper 85-1769-CP, Snowmass, CO, Aug. 1985, pp. 1-33.
4. Robinson, M.C. and Luttges, M.W., "Unsteady Flow Separation and Attachment Induced by Pitching Airfoils," AIAA Paper 83-0131, Reno, Nev., Jan. 1985, pp. 1-12.
5. Robinson, M.C. and Luttges, M.W., "Vortex Generation Induced by Oscillating Airfoils; Maximizing Flow Attachment," VIII Biennial Symposium on Turbulence, University of Missouri, Rolla, 1983, pp. 117-126.
6. Robinson, M.C. and Luttges, M.W., "Unsteady Separated Flow: Forced and Common Vorticity about Oscillating Airfoils," Workshop on Unsteady Separated Flows, Francis, M. and Luttges, M. (eds.), Univ. of Colorado, Boulder, 1983, pp. 117-126.
7. McAlister, K.W., and Carr, L.W., "Water Tunnel Visualizations of Dynamic Stall", J. Fluids Engr., Vol. 101, 1979, pp. 376-380.
8. McCroskey, W.J., Carr, L.W., and McAlister, K.W., "Dynamic Stall Experiments on Oscillating Airfoils," AIAA Paper No. 75-125, Jan. 1975.
9. Carr, L.W., McAlister, K.W., and McCroskey, W.J., "Analysis of the Development of Dynamic Stall Based on Oscillating Airfoil Experiments," NASA TN-8382, Jan. 1977.
10. Walker, J.M., Helin, H.E., and Strickland, J.H., "An Experimental Investigation of an Airfoil Undergoing Large Amplitude Pitching Motions," AIAA Journal, Vol. 23, Aug. 1985, pp. 1141-1142.
11. Walker, J.M., Helin, H.E., and Chou, D.C., "Unsteady Surface Pressure Measurements on a Pitching Airfoil," AIAA Paper 85-0532, Boulder, CO., Mar. 1985, pp. 1-10.
12. Francis, M.S., and Keesee, J.E., "Airfoil Dynamic Stall Performance With Large-Amplitude Motions", AIAA Journal, Vol. 23, Nov. 1985, pp. 1653-1659.
13. Luttges, M.W., Robinson, M.C., and Kennedy, D.A., "Control of Unsteady Separated Flow Structures on Airfoils", AIAA Paper 85-0531, Boulder, CO., Mar. 1985, pp. 1-12.
14. Viets, H., Palmer, M.G., and Bethke, R.J., "Potential Applications of Forced Unsteady Flows," Workshop on Unsteady Separated Flows, Francis, M. and Luttges, M. (eds.), Univ. of Colorado, Boulder, 1983, pp. 21-27.
15. Robinson, M.C., and Luttges, M.W., "Vortices Produced By Air Pulse Injection From the Surface of an Oscillating Airfoil", AIAA Paper 86-0118, Reno, Nev., Jan. 1986, pp. 1-13.
16. Helin, H.E., Robinson, M.C., and Luttges, M.W., "Visualization of Dynamic Stall Controlled by Large Amplitude Interrupted Pitching Motions", AIAA Paper 86-2281-CP, Williamsburg, VA., Aug. 1986, pp. 1-18.
17. Adler, J.N., and Luttges, M.W., "Three-Dimensionality in Unsteady Flow About a Wing," AIAA Paper 85-0132, Reno, Nev., Jan. 1985, pp. 1-6.
18. Gad-el-Hak, M., and Ho, C-M., "The Pitching Delta Wing", AIAA Journal, Vol. 23, Nov. 1985, pp. 1660-1665.
19. Ashworth, J., Waltrip, M., and Luttges, M.W., "Three-Dimensional Unsteady Flow Fields Elicited by a Pitching Forward Swept Wing", AIAA Paper No. 86-1104, May 1986.
20. Adler, J.N., Robinson, M.C., Luttges, M.W., and Kennedy, D.A., "Visualizing Unsteady Separated Flows," III International Symposium on Flow Visualization, 3, 1983, pp. 806-811.
21. Junper, E.J., Shreck, S.J., and Dimmick, R.L., "Lift Curve Characteristics for an Airfoil Pitching at Constant Rate", AIAA Paper 86-0117, Reno, Nev., Jan. 1986, pp. 1-10.

END

DTIC

7-86